RSC Advances

ROYAL SOCIETY OF CHEMISTRY

www.rsc.org/advances

Microstructural, Rheological, and Antibacterial Properties of Cross-linked Chitosan Emulgels

Lingling Lei[1], Zongze He[1], Huanle Chen[1], David Julian McClements[3,4], Bin Li[1,2], Yan Li[1,2]*

1. College of Food Science and Technology, Huazhong Agricultural University, Wuhan 430070, China

2. Key Laboratory of Environment Correlative Dietology (Huazhong Agricultural University), Ministry of Education, China

3. Department of Food Science, University of Massachusetts, Amherst, MA 01003, USA

4. Department of Biochemistry, Faculty of Science, King Abdulaziz University, Jeddah, Saudi Arabia

Journal: *RSC Advances*

Running title: *Chitosan based emulgel by incorporating essential oil nanoemulsions*

* Corresponding author. Address: No 1 Shizishan Road, Hongshan District, Wuhan 430070, China, E-mail: yanli@mail.hzau.edu.cn, Phone: +86 27 87282111, Fax: +86 27 87282111

ABSTRACT

Antimicrobial emulgels were fabricated by cross-linking chitosan using cinnamaldehyde (CA) nanoemulsions. The influence of system composition and pH on the properties of the emulgels was characterized using electron and confocal fluorescence microscopy, dynamic shear rheology, and Fourier transform infrared spectroscopy (FTIR). FTIR confirmed the occurrence of a Schiff base reaction between chitosan and CA. Rheology measurements helped establish the optimum pH and system composition required to fabricate emulgels. Microscopy provided information about the network structure formed within lyophilized emulgels. The emulgels were shown to have strong antibacterial activity against *E. coli* and *S. aureus*.

Keywords: Chitosan; cinnamaldehyde; nanoemulsions; Schiff base; hydrogel;

INTRODUCTION

Emulgels are biphasic formulations whose internal phase is an emulsified non-polar liquid (usually oil) and whose external phase is a semisolid polar liquid (usually water) [1]. Since they have polar, non-polar, and interfacial regions they can be used to encapsulate hydrophilic, lipophilic, and amphiphilic substances. For certain applications, emulgel-based delivery systems have advantages over conventional emulsion-based delivery systems, *e.g.,* where high physical stability, novel rheological properties, or controlled release properties are required. In the pharmaceutical industry, both lipophilic and hydrophilic drugs have been loaded into emulgels designed for topical delivery, such as mefenamic acid [2], insulin [3], itraconazonle, aceclofenac [4], calcipotriol [5], diclofenac [6], and ciprofloxacin, [7]. Many of the delivery systems fabricated in the pharmaceutical industry are based on components that cannot be utilized within the food industry, such as specific synthetic polymers and surfactants. However, studies have shown that emulgels can be fabricated from natural food-grade materials, such as biopolymers [8].

Natural polymers have been extensively exploited for developing formulations for biomedical and food applications. Chitosan is a polysaccharide that has a number of characteristics that make it particularly suitable for fabricating structured delivery systems, including positive charge, biocompatibility, biodegradability, mucoadhesion, and antibacterial activity [9-11]. Chitosan-based biomaterials have therefore been widely utilized to construct delivery systems in both the food and pharmaceutical industries [12,

[13].

Cinnamaldehyde (CA) is an aromatic aldehyde that is a major component of the bark extract of cinnamon [14]. It has been approved by the FAO/WHO Expert Committee on Food Additives (JECFA) for use as a food-flavoring agent [15]. CA has been shown to be a highly effective natural antimicrobial agent, with activity against a broad range of food-borne pathogens and spoilage organisms [14, 16]. Recent studies have reported that CA cross-linked chitosan materials can be designed as nanoparticles [17], hydrogels [18], and films [19-21]. For example, chitosan nanoparticles have been fabricated by an emulsion-templating method using CA as a crosslinking agent [22]. In this case, the chitosan was present in the inner phase and the CA was present in the outer phase of a water-in-oil emulsion. Chitosan microparticles have also been formed by mixing a CA acetone solution with a chitosan solution [18].

In the current study, chitosan-based emulgels were fabricated by mixing CA nanoemulsions with chitosan solutions. In these systems, the CA acted as an emulsified antimicrobial oil phase, as well as a cross-linking agent for the chitosan. The aldehyde groups in this essential oil can cross-link the amino groups in chitosan through a Schiff base reaction. The emulgels formed were characterized by microscopy, rheology, and spectroscopy to obtain some insight into their properties and structure. In addition, the antibacterial activity of the emulgels was evaluated against Gram-positive microorganisms (*S. aureus*) and Gram-negative ones (*E. coli*). To the authors' knowledge, this is the first report on the antimicrobial activity of

chitosan-based emulgels that contain CA nanoemulsions contained within covalently cross-linked hydrogels.

MATERIALS AND METHODS

Materials

Chitosan (degree of deacetylation of 85%; viscosity of 1 % chitosan solution at 20 ^{o}C or 1250 mPa.s) was gifted by Zhejiang Golden-Shell Pharmaceutical Co. (Zhejiang, China). Cinnamaldehyde (≥ 95%, CA) and analytical reagent grade acetic (AA) were purchased from Aladdin Reagent Co. (Shanghai, China). Medium chain triglycerides (MCT, ≥ 95%) were obtained from Wuhan Boxing Chemical Co. (Wuhan, China). Tween 80, hydrochloric acid (HCl) and sodium hydroxide (NaOH) were purchased from Sinopharm Chemical Reagent Co. (Shanghai, China). Distilled water (electrical resistance ≈ 18.2 MΩ·cm) was used to prepare all aqueous solutions. All the other chemicals were of analytical grade.

Nutrient Broth (NB) was purchased from Qingdao Hope Bio-Technology Co.,Ltd. Agar was purchased from Sigma-Aldrich (WUXI) Life Science & Tenchnolgy Co., Ltd. *Escherichia coli* (*E. coli*) and *Staphylococcus aureus* (*S. aureus*) were obtained from China Center for Type Culture Collection, Wuhan University (Wuhan, China).

Formation of chitosan-based emulgels

Cinnamaldehyde-loaded nanoemulsion preparation

The formation of CA nanoemulsions was carried out using the spontaneous emulsification method described previously [23]. Briefly, an organic phase was added dropwise into an aqueous phase at ambient temperature while continuously stirring at 600 rpm using a magnetic stirrer for 15 min. The organic phase consisted of a mixture of CA, MCT, and Tween 80 with the mass ratio at 1:1:1.5, while the aqueous phase consisted of distilled water. The total oil phase (MCT + CA) was maintained at 10 wt% while the surfactant (Tween 80) was maintained at 10%. The nanoemulsion was diluted before mixing with chitosan solution.

Chitosan solution preparation

Chitosan powder (1.0 g) were dispersed into 99.0 g of 1 v/v% acetic acid solution at room temperature, which was mechanically stirred overnight, and then centrifuged at a speed of 3500 rpm for 15 min to remove any air bubbles or other impurities.

Gel preparation

CA cross-linked chitosan gels were prepared by mixing equal volumes of CA nanoemulsions and chitosan solutions. The concentration of chitosan was fixed at 1 wt% and the content of CA in the nanoemulsions was varied from 0.25% to 5%. The corresponding molar ratios between –CHO and -NH_2 therefore shifted from 0.19 to

3.71. Here, -CHO and -NH_2 refer to the carbonyl group on the CA molecules and the amino groups on the chitosan molecules, respectively. After 10 min of stirring, the uniform gel-forming solutions were obtained with initial pH around 3.8-4.0. Then pH values of the gel-forming solutions were adjusted from 4.3 to 4.4, 4.5, or 4.6. When the pH was higher then 4.6, some of the mixtures formed a gel so quickly that the pH could not be adjusted any more, and therefore these higher pH values were not used. After the adjustment of pH, the mixtures were stored at room temperature (around 25 ^{o}C) to form gels. It should be noted that chitosan solution alone did not form gels under similar conditions, indicating that the essential oil was necessary for cross-linking. Some of the gels were frozen-dried and stored in an amber glass desiccator with P_2O_5 at ambient temperature (around 23 °C) prior to use.

Characterization of chitosan films

Fourier-transform infrared spectroscopy (FTIR)

Fourier transform infrared spectra of dried chitosan films were recorded using a FTIR spectroscopy instrument (FT-IR 615, Japan). The dried samples were ground into powders, mixed with KBr, and then pressed to form a disk for the tests.

Microstructure

Scanning electronic microscopy (SEM): The morphology of the surface and cross-section of the films was examined using scanning electron microscopy (SEM, Hitachi S-4500, Japan) at an accelerated electron energy of 30 keV.

Confocal microscopy: A Nikon Confocal Microscope (C1 Digital Eclipse, Tokyo, Japan) with a 60 × oil immersion objective lens was used to capture the confocal images. Nile red (a fat soluble fluorescent dye) was excited using a 488 nm argon laser. The fluorescence emitted from the sample was monitored using a fluorescence detector (515/30) with a pinhole size of 150 μm. The resulting images consisted of 512 × 512 pixels, with a pixel size of 414 nm, and a pixel dwell time of 61.44 μs. Nile red was added into nanoemulsions before mixing with chitosan solution. Then pH was adjusted into 4.6. One drop of the mixture was put in the glass slide and covered prior to the formation of the gels.

Rheology

The rheological behavior of gels containing different amounts of CA was characterized by dynamic shear rheology. Initially, the linear viscoelastic region was established using strain-sweep experiments. Then, the storage modulus (G') and loss modulus (G") were measured as functions of time using a strain of 2% and frequency of 0.01 Hz. The rheological properties were measured as a function of time after mixing the chitosan solution and nanoemulsion to determine the influence of CA content and pH values (25.0 ± 0.2 ^{o}C). The dynamic shear rheology was measured until the storage modulus 1 Pa, and then an oscillatory frequency sweep (0.01 to 100 Hz) was carried out. All experiments were conducted using a rheometer (TA-AR2000ex, UK) with a parallel-plate geometry (40 mm in diameter, gap in 1 mm).

Antibacterial assay

The antibacterial efficacy of the emulgels was tested using a disk-diffusion method. Gram-negative bacteria *E. coli* and Gram-positive bacteria *S. aureus* were selected as representative microorganisms. To perform this experiment, the emulgels were prepared in a cylindrical mold made by silver paper with a diameter of approximately 13 mm. After the formation of the gels, silver papers were peeled away. The cylindrical emulgels were covered on the surface of the nutrient agar in Petri dishes which were inoculated with 100 μL bacterial solution taken from a diluted nutrient broth medium. The concentration of bacteria solutions was approximately 10^8 CFU/mL, counted using the method of standard plate count. After being incubated at 37 °C for 24 h, the inhibition zones were measured with a tolerance of 1 mm. The experiment was repeated three times for each sample. Saline, chitosan, and CA solutions were evaluated as controls.

Release and retention of cinnamaldehyde

2 g of gelling solution was kept in the tube containing 2.0 mL normal saline solution (0.9 w/v% NaCl) with virtually no headspace. 1 mL of normal saline was collected at different time intervals for analysis. The retention of CA was monitored by directly measuring CA concentration in the alcohol solution and nanoemulsion as a function of time. CA concentration was determined by using Uv-vis spectrometry (UV-1800, Shimadzu, Japan) at an absorbance of 291 nm. A standard curve was prepared prior to the measurement.

Statistical analysis

All experiments were performed in triplicate on freshly prepared samples. The results were then reported as averages and standard deviations of these measurements.

RESULTS AND DISCUSSIONS

Preparation of chitosan-based emulgels

Chitosan alone did not form gels after dissolution in acetic acid solutions because it is fully protonated at these low pH values and so there is a strong electrostatic repulsion between the cationic polysaccharide molecules. When chitosan solutions were simply mixed with CA nanoemulsions no gelation was observed, which was attributed to the fact that the pH of the resulting mixture was relatively low (3.8 to 4.0). However, once the pH was adjusted to 4.6, the viscosity of the mixture gradually increased and then the system formed a gel. Hence, the influence of CA content on the formation of emulgels was studied at pH 4.6 (Table 1). The fact that the hydrophobic CA was encapsulated in oil-in-water nanoemulsions meant that the cross-linking agent could easily be homogenously distributed throughout the chitosan solutions, which would be expected to favor the formation of more uniform gels. The addition of the nanoemulsion to the chitosan solution led to an increase in the turbidity of the overall system, which can be attributed to some light scattering by the lipid droplets in the nanoemulsion. After the formation of emulgels, the color of the overall system because an opaque white, with the lightness depending on CA content

(Fig. 1). When the number of aldehyde groups (-CHO from CA) was less than the amino groups (-NH_2 from chitosan), it took longer time for the conversion of the fluid mixture into a gel. At the highest CA content, it only took around 1 min to form a strong gel, while at the lowest CA content only a viscous liquid could be formed (Table 1). The lightness of the gels also increased with increasing CA content (Fig. 1), indicating a change in their microstructure.

FTIR spectrophotometric analysis

There were appreciable differences in the FTIR spectra of dried chitosan and dried chitosan emulgels (Fig. 2), which suggests that imine bond formation and other structural modifications had occurred. For the pure chitosan powder: the peaks in the range 3800 – 2600 cm^{-1} were assigned to different –OH stretching vibrations corresponding to intra- and inter- molecular H-bonds; the peak at 3430 cm^{-1} was assigned to -NH and -OH stretching vibrations; and, the peaks observed at 2926 and 2856 cm^{-1} were assigned to symmetric and antisymmetric -CH_2 stretching vibrations (Fig. 2). The peaks observed in the spectra of chitosan powder at wavenumbers of 1656, 1542 and 1422 cm^{-1} were assigned to -C=O (amide I), NH (amide II), and HN-CO (amide III) stretching vibrations, respectively [24-26], while the broad absorption peak at 1085 cm^{-1} was assigned to C-O stretching. After the formation of emulgels, the peaks in the range 3800 – 2600 cm^{-1} became narrow and there was a slight shift in the wavenumbers corresponding to the peaks, but with an increase in the peak

intensities at 2926 and 2856 cm^{-1}. In comparison to the spectra of the pure chitosan, the powdered emulgels had some distinctive peaks at 688, 748, 1455 cm^{-1} (Fig. 5), which corresponded to the phenyl group of CA [18]. The band at 1656 cm^{-1} shifted into 1636 cm^{-1}, indicating the formation of the imine group (C=N) by Schiff base [27]. The shift of peak 1542 cm^{-1} to 1574 cm^{-1} could be attributed to the chitosan or surfactant (Tween 80) [28]. The new peak at 1741 cm^{-1} could be assigned as –O–C=O, due to the existence of surfactant (Tween 80), which became slight sharper with higher nanoemulsion content. Overall, FTIR profiles of all the emulgels were similar.

Rheological properties of emulgels

The dynamic shear moduli (G' and G'') for chitosan/nanoemulsion mixtures with different CA contents and pH values were measured (Fig. 3). At the lowest CA concentration (0.25%, pH 4.6), the values of G' and G'' were very low and G'' was always slightly higher than G', indicating that gelation did not occur, which is consistent with visual observations (Fig. 1). As the CA content was increased, a crossover between G' and G'' was observed during the gelation process (*i.e.,* G' became greater than G''), indicating that gelation occurred, which is again consistent with the visual observations. The gelation time, defined as the point where G' first exceeded 1 Pa [29-31], decreased with increasing CA content *i.e.,* higher nanoemulsion content (Fig. 3b, left). This effect can be attributed to the fact that the gelation rate and extent increased as the molar ratio of aldehyde to amino groups increased. Presumably,

a three-dimensional network of covalently cross-linked chitosan molecules is formed that traps the small lipid droplets from the nanoemulsion. The gelation time and final G' values also depended on the environmental pH values: gelation was quicker and the final G' value was larger for higher pH values. After gelation, the influence of oscillation frequency on the rheological response of the emulgels was investigated (Fig. 3b, right). In the low frequency regime, the samples behaved as viscoelastic solids (G'> G"), but above a certain frequency G" became higher than G', indicating the samples exhibited more viscous character. As the CA content increased, the critical frequency required to reach this crossover point increased (Fig. 1S).

Microstructure of emulgels

The microstructure of freeze-dried chitosan-based emulgels depended on CA content (Fig. 4). At low CA levels (A and B), the surface of the emulgels had an open network structure containing relatively large pores. These large pores were not observed when the CA content was ≥ 1%. (C, D and E), indicating that a more homogeneous network structure had been formed in these gels. Nevertheless, the surfaces of these gels did have a wrinkled/rough appearance. Microscopy images of the cross-section of emulgels formed using a CA content of 0.25% had similar network structures as observed at the surface. At higher CA contents, the cross-sections of the emulgels exhibited a more laminated structure. When the CA content was 1% or 1.5%, the layered structure was relatively open, but at higher levels

it became more compact. Enlarged images (insets) indicated that there were numerous small particles attached to the layers, which were probably lipid droplets. The structure observed in the present work was different from the that of chitosan and CA hydrogels reported previously, which had porous sponge-like microstructures after drying [18]. However, these hydrogels were formed by mixing chitosan solution with CA acetone solution rather than with CA nanoemulsions.

To further confirm the location of the CA droplets within the emulgels, the microstructure was observed by confocal microscopy using a lipid-soluble fluorescent dye to identify the location of the oil phase (Fig. 5). In this case, the samples were analyzed in their wet state (without dehydration). These measurements indicated that the nanoemulsion droplets were distributed throughout the gel network. At low nanoemulsion concentrations, the network structure was irregular and loose, while at higher concentrations it was more compact and uniform. Interestingly, the confocal microscopy images also suggested that a laminar structure was formed within the emulgels.

The proposed mechanism for the formation and structure of the chitosan and CA emulgels is summarized in Fig. 6. The cross-linking of the chitosan molecules is likely to occur due to a Schiff base reaction between chitosan and CA occurring near the surface of the nanoemulsion droplets. At low CA contents, there are insufficient cross-links to form a homogeneous polymer network throughout the system, which leads to the formation of a structure containing large pores that does not gel. On the

other hand, at high CA contents there are sufficient cross-links to form a homogenous network throughout the sample, leading to the formation of a gel with a relatively fine structure..

Antibacterial activity of emulgels

A disk inhibition test was performed to evaluate the antimicrobial activities of CA and CA-loaded emulgels against *E. coli* and *S. aureus*. CA dissolved in alcohol was used as a control to investigate the antimicrobial properties of CA nanoemulsions and chitosan-based emulgels. Fig. 7 shows the inhibition zone of different systems with an equal level of CA. The antibacterial activity of CA was dose-independent. The CA dissolved in alcohol was unable to create an inhibition zone around the sheet or had the smallest inhibition zone. CA nanoemulsions had higher antibacterial activities than the CA solution. However, CA-loaded emulgels gave the biggest inhibition zone, indicating that they were the most effective antimicrobial systems. At 2.5% CA, the inhibition zones of the solution, nanoemulsion and emulgel were 3.67, 8.47, 20.74 mm and 3.67, 9.57, 29.77 mm for *E. coli* and *S. aureus*, respectively. Interestingly, increasing the level of the CA in the nanoemulsions or emulgels did not lead to an appreciable increase in their antimicrobial efficacy (Fig. 7). In addition, the emulgels were more difficult to form and tend to shrink and exude fluid, probably because of the greater extent of cross-linking. Consequently, there was little advantage to including higher levels of CA in the emulgels. Similar observations have been

reported in other studies using CA as a cross-linking agent [32]. The release of CA from emulgels was further studied as shown in Fig. 8. It indicated that the release of CA from emulgels was faster within 24 h and then became slow, independent on the formulation. At the low CA level, the release rate of CA was more than 50% after 96 h, which was much higher than that at the high CA level. The retention of CA in alcohol solution and nanoemulsion were higher than 90% within 48 h (**Data now shown**), which is consistent with our previous results [23]. The stability of CA in nanoemulsion was evaluated by electronic nose that nanoemulsion could slow the evaporation of CA. Initial CA concentration had slight effect on its retention in solution or emulsion.

CONCLUSIONS

The study reports the successful development of antimicrobial emulgels formed by using CA nanoemulsions to cross-link chitosan molecules. In these systems, the CA acts as both a cross-linking agent and an antimicrobial agent. FTIR results demonstrated that a Schiff base reaction was involved in the formation of the emulgels between aldehyde groups from the CA and amino groups from the chitosan. The pH and CA concentration had to be controlled to successfully produce emulgels. The gelation time decreased, gel strength increased, and gel uniformity increased with increasing CA concentration. Microscopy measurements suggested that the nanoemulsion droplets containing the CA were embedded in the polymer network of the emulgels. CA-loaded emulgels had higher antibacterial activity than CA solutions or nanoemulsions. Chitosan-based emulgels can be fabricated from natural food-grade

ingredients, and are easy to prepare and handle, and so they may have applications as antimicrobial treatments in food preservation.

ACKNOWLEDGMENTS

This work was financially supported by National Natural Science Foundation of China (No. 31401528), Natural Science Foundation of Hubei Province of China (No. 2014CFB326) and National Science-technology Support Plan Projects (No. 2015BAD16B06).

The authors have no declared conflict of interest.

REFERENCES

1. Ajazuddin, A. Alexander, A. Khichariya, S. Gupta, R. J. Patel, T. K. Giri and D. K. Tripathi, *Journal of Controlled Release*, 2013, **171**, 122-132.

2. R. Khullar, D. Kumar, N. Seth and S. Saini, *Saudi pharmaceutical journal : SPJ : the official publication of the Saudi Pharmaceutical Society*, 2012, **20**, 63-67.

3. M. Akram, S. B. Naqvi and A. Khan, *Pakistan journal of pharmaceutical sciences*, 2013, **26**, 323-332.

4. K. C. Ashara, J. S. Paun, M. M. Soniwala, J. R. Chavada and N. M. Mori,

Asian Pacific Journal of Tropical Disease, 2014, **4**, S27-S32.

5. V. Naga Sravan Kumar Varma, P. V. Maheshwari, M. Navya, S. C. Reddy, H. G. Shivakumar and D. V. Gowda, *Saudi pharmaceutical journal : SPJ : the official publication of the Saudi Pharmaceutical Society*, 2014, **22**, 591-599.

6. C. Yang, Y. Shen, J. Wang, A. Ouahab, T. Zhang and J. Tu, *Drug delivery*, 2014, DOI: 10.3109/10717544.2014.898111.

7. S. S. Sagiri, V. K. Singh, S. P. Mallick, A. Anis, S. M. Al-Zahrani, D. Pradhan, K and K. Pal, *International Journal of Electrochemical Science*, 2015, **10**, 1233-1248.

8. S. Wakhet, V. K. Singh, S. Sahoo, S. S. Sagiri, S. Kulanthaivel, M. K. Bhattacharya, N. Kumar, I. Banerjee and K. Pal, *Journal of materials science. Materials in medicine*, 2015, **26**, 118.

9. R. Muzzarelli, M. Mehtedi and M. Mattioli-Belmonte, *Marine Drugs*, 2014, **12**, 5468.

10. J. Lišková, T. E. L. Douglas, J. Beranová, A. Skwarczyńska, M. Božič, S. K. Samal, Z. Modrzejewska, S. Gorgieva, V. Kokol and L. Bačáková, *Carbohydrate Polymers*, 2015, **129**, 135-142.

11. R. A. Muzzarelli, F. Greco, A. Busilacchi, V. Sollazzo and A. Gigante, *Carbohydr Polym*, 2012, **89**, 723-739.

12. L. Casettari and L. Illum, *Journal of Controlled Release*, 2014, **190**, 189-200.

13. V. A. Pereira Jr, I. N. Q. de Arruda and R. Stefani, *Food Hydrocolloids*, 2015, **43**, 180-188.

14. S. Burt, *International Journal of Food Microbiology*, 2004, **94**, 223-253.

15. J. Cocchiara, C. S. Letizia, J. Lalko, A. Lapczynski and A. M. Api, *Food Chem Toxicol*, 2005, **43**, 867-923.

16. R. A. Holley and D. Patel, *Food Microbiology*, 2005, **22**, 273-292.

17. V. Nipun Babu and S. Kannan, *Int J Biol Macromol*, 2012, **51**, 1103-1108.

18. L. Marin, S. Moraru, M. C. Popescu, A. Nicolescu, C. Zgardan, B. C. Simionescu and M. Barboiu, *Chemistry (Weinheim an der Bergstrasse, Germany)*, 2014, **20**, 4814-4821.

19. L. Higueras, G. López-Carballo, R. Gavara and P. Hernández-Muñoz, *Food Bioprocess Technol*, 2015, **8**, 526-538.

20. L. Marin, I. Stoica, M. Mares, V. Dinu, B. C. Simionescu and M. Barboiu, *Journal of Materials Chemistry B*, 2013, **1**, 3353-3358.

21. K. A. Rieger, N. M. Eagan and J. D. Schiffman, *Journal of Applied Polymer Science*, 2015, **132**.

22. V. Nipun Babu and S. Kannan, *International Journal of Biological Macromolecules*, 2012, **51**, 1103-1108.

23. W.L. Tian, L.L. Lei, Q. Zhang and Y. Li, *Journal of Food Process Engineering*,

2015, DOI: 10.1111/jfpe.12237, n/a-n/a.

24. J. Brugnerotto, J. Lizardi, F. M. Goycoolea, W. Arguelles-Monal, J. Desbrieres and M. Rinaudo, *Polymer*, 2001, **42**, 3569-3580.

25. J. M. Lagaron, P. Fernandez-Saiz and M. J. Ocio, *Journal of Agricultural and Food Chemistry*, 2007, **55**, 2554-2562.

26. K. Ziani, J. Oses, V. Coma and J. I. Maté, *LWT - Food Science and Technology*, 2008, **41**, 2159-2165.

27. L. Higueras, G. López-Carballo, R. Gavara and P. Hernández-Muñoz, *Food and Bioprocess Technology*, 2014, **8**, 526-538.

28. J. Grant, J. Cho and C. Allen, *Langmuir : the ACS journal of surfaces and colloids*, 2006, **22**, 4327-4335.

29. J. A. Lucey, M. Tamehana, H. Singh and P. A. Munro, *Food Research International*, 1998, **31**, 147-155.

30. A. Tobitani and S. B. Ross-Murphy, *Macromolecules*, 1997, **30**, 4845-4854.

31. Y. L. Tan, A. Ye, H. Singh and Y. Hemar, *Journal of Texture Studies*, 2007, **38**, 404-422.

32. K. A. Rieger and J. D. Schiffman, *Carbohydr Polym*, 2014, **113**, 561-568.

Table 1 Gel formation of CA emulsion mixed with 1.0% chitosan at pH 4.6

CA content%	**0.25%**	**0.5**	**1**	**2**	**3**	**4**	**5**
CHO : NH_2	0.19	0.37	0.74	1.49	2.23	2.97	3.71
Color	Opaque	Opaque	Opaque /white	Opaque /white	White	White	White
Gelling time (min) by visual observation	max	204	26	21	15	3	1

Figure Captions

Fig. 1. Pictographs of chitosan-based emulgels. Chitosan concentration was fixed at 0.5 wt%. From left to right with decreasing CA nanoemulsion content in nanoemulsion

Fig. 2. FTIR Spectra of chitosan powder (CS) and emulgels with selected formulations. CSG1: 0.25 wt% CS + 0.5% emulsion, CSG2: 0.5 wt% CS + 1% emulsion, CSG3: 0.5 wt% CS + 2% emulsion, CSG4: 0.5 wt% CS + 3% emulsion, CSG5: 0.5 wt% CS + 5% emulsion.

Fig. 3a. Rheological properties of chitosan-based emulgels under different CA nanoemulsion contents ((A) 0.25%, (B) 0.5%, (C) 1%, (D) 2%, (E) 5%) at the same pH of 4.6 and pHs ((F) 4.4, (G) 4.5, (H) 4.6) at the same CA nanoemulsion content of 1%. Chitosan concentration in all the emulgels was 0.5 wt%. G': Solid square, G'': Open square

Fig. 3b. Plots of time when G'= 1 Pa and evolution of G' as a function of frequency after the gelation point. Chitosan concentration in all the emulgels was 0.5 wt% and CA nanoemulsion contents varied: (A) 0.5%; (B) 1%; (C) 2%; (D) 3%; (E) 4%; (F) 5%

Fig. 4. Surface and cross-section microstructure of dried emulgels, chitosan concentration in all the emulgels was 0.5 wt% and CA nanoemulsion contents varied: (A) 0.5%; (B) 1%; (C) 2%; (D) 3%; (E) 4%; (F) 5%

Fig. 5. Confocal microscopy of wet emulgels, chitosan concentration in all the emulgels was 0.5 wt% and CA nanoemulsion contents varied: (A) 0.5%; (B) 1%; (C) 2%; (D) 5%

Fig. 6. Scheme of (A)chitosan and CA nanoemulsions emulgels Formation and (B) network microstructure of emulgels under different CA content and after

freeze-drying

Fig. 7. Antibacterial activity against *E. coli* (A and A') and *S. aureus* (B and B') of emulgels with different amount of CA and MCT ratio in the formulation of nanoemulsions. A, B: the mass ratio of CA to MCT is 1:1, A' and B': the mass ratio of CA to MCT is 2:1

Fig. 8. Influence of CA level on the cumulative release of CA from chitosan emulgels containing different amount of CA and MCT ratio in the formulation of nanoemulsions. Formulation 1: the mass ratio of CA to MCT is 2:1, Formulation 2: the mass ratio of CA to MCT is 1:1

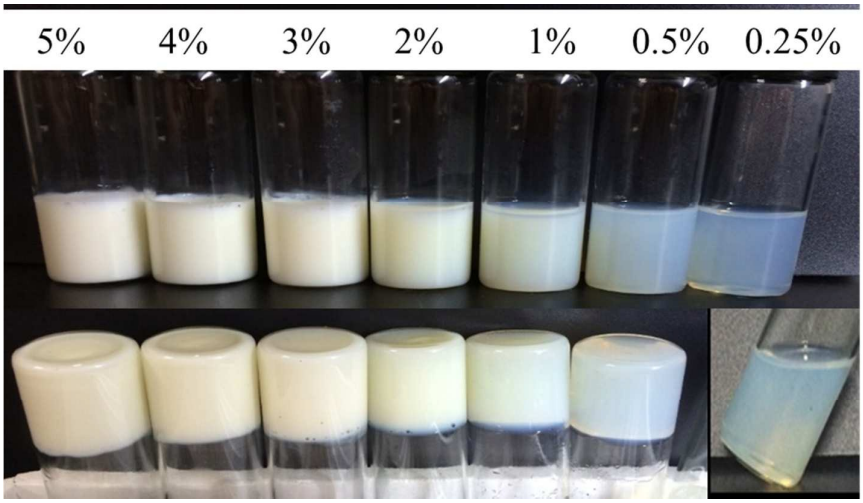

Fig. 1. Pictographs of chitosan-based emulgels. Chitosan concentration was fixed at 0.5 wt%. From left to right with decreasing CA nanoemulsion content in nanoemulsion

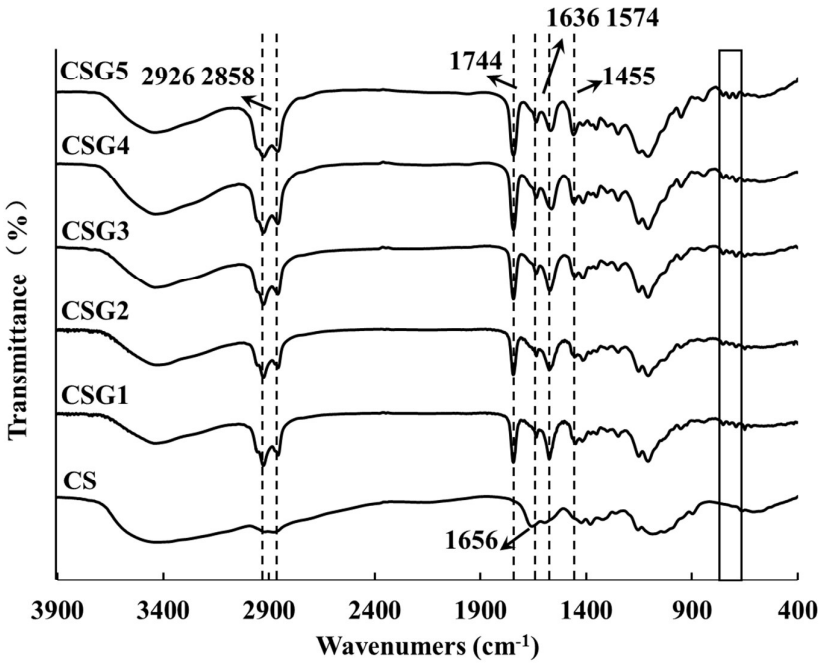

Fig. 2. FTIR Spectra of chitosan powder (CS) and emulgels with selected formulations. CSG1: 0.25 wt% CS + 0.5% emulsion, CSG2: 0.5 wt% CS + 1% emulsion, CSG3: 0.5 wt% CS + 2% emulsion, CSG4: 0.5 wt% CS + 3% emulsion, CSG5: 0.5 wt% CS + 5% emulsion.

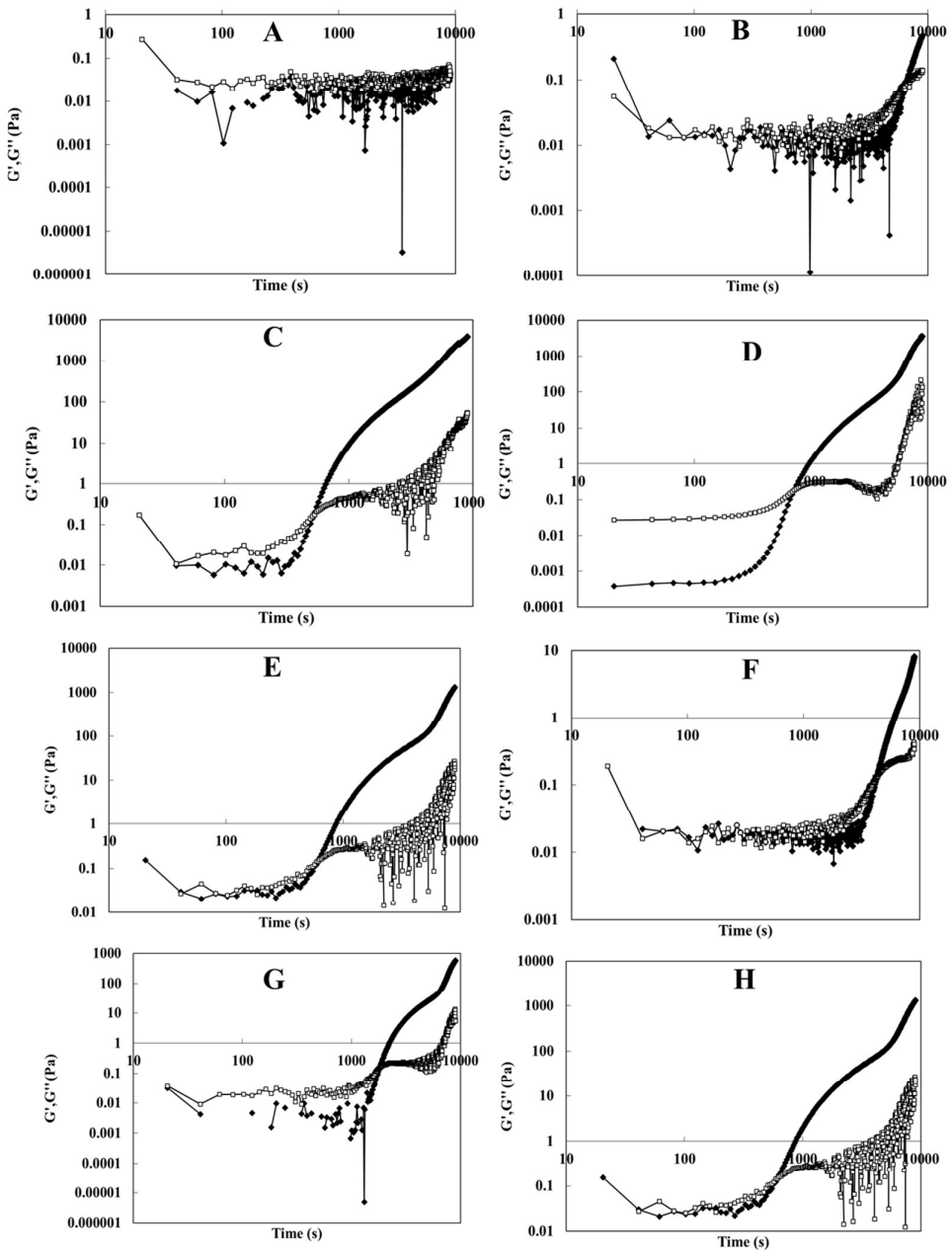

Fig. 3a. Rheological properties of chitosan-based emulgels under different CA nanoemulsion contents ((A) 0.25%, (B) 0.5%, (C) 1%, (D) 2%, (E) 5%) at the same pH of 4.6 and pHs ((F) 4.4, (G) 4.5, (H) 4.6) at the same CA nanoemulsion content of 1%. Chitosan concentration in all the emulgels was 0.5 wt%. G': Solid square, G'': Open square

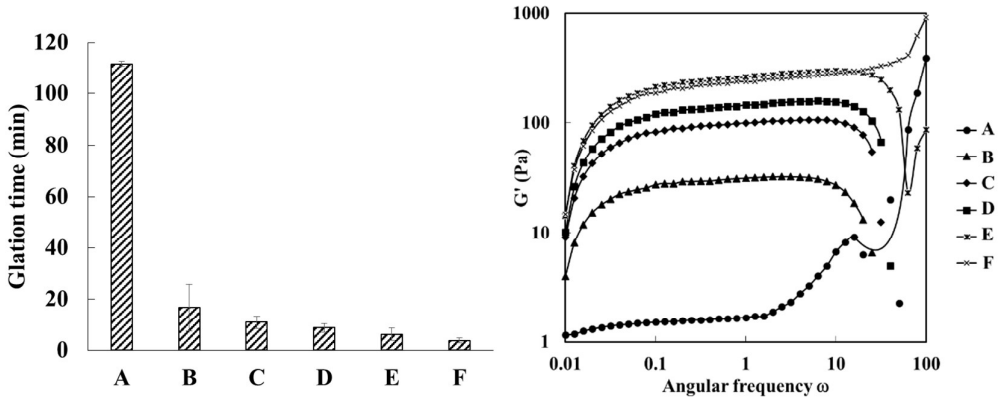

Fig. 3b. Plots of time when G'= 1 Pa and evolution of G' as a function of frequency after the gelation point. Chitosan concentration in all the emulgels was 0.5 wt% and CA nanoemulsion contents varied: (A) 0.5%; (B) 1%; (C) 2%; (D) 3%; (E) 4%; (F) 5%

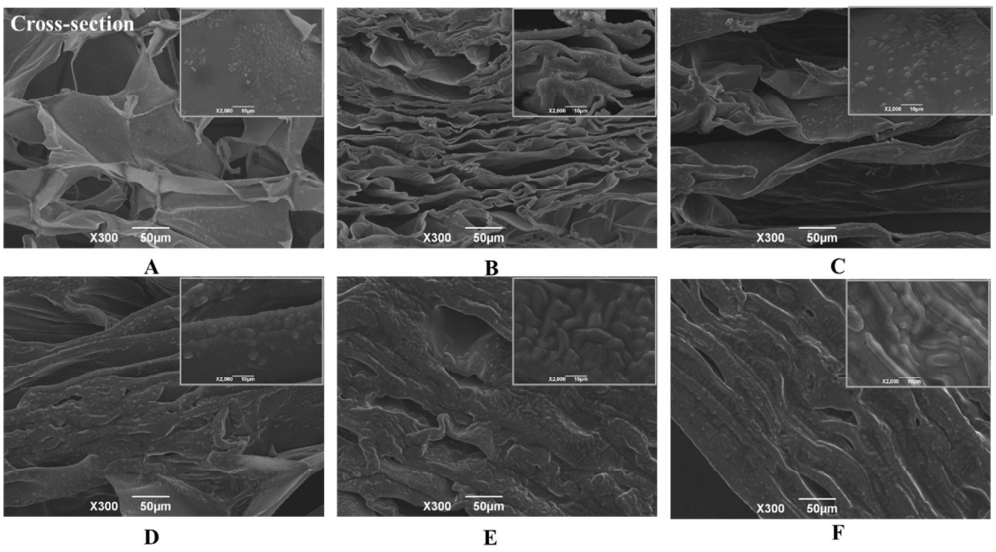

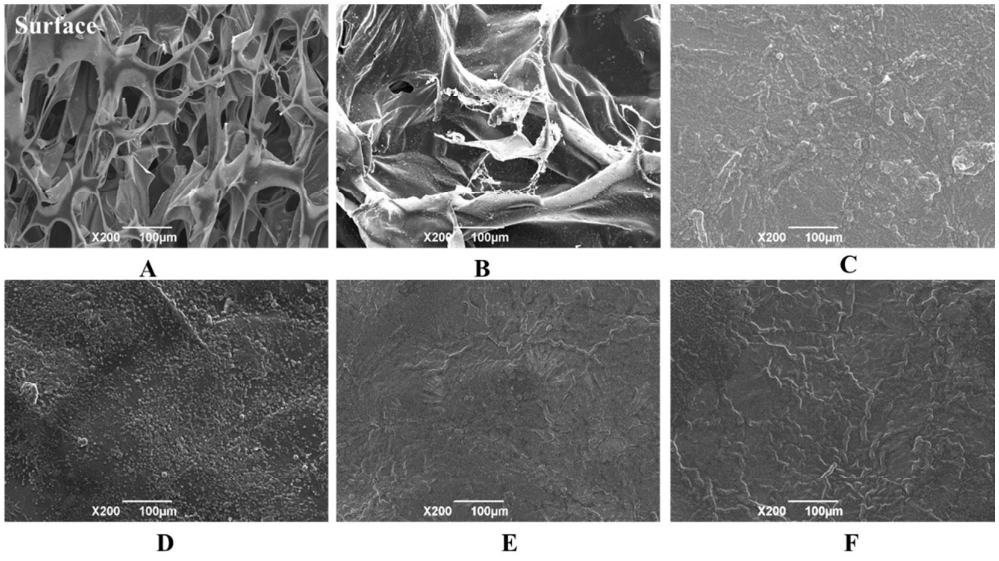

Fig. 4. Surface and cross-section microstructure of dried emulgels, chitosan concentration in all the emulgels was 0.5 wt% and CA nanoemulsion contents varied: (A) 0.5%; (B) 1%; (C) 2%; (D) 3%; (E) 4%; (F) 5%

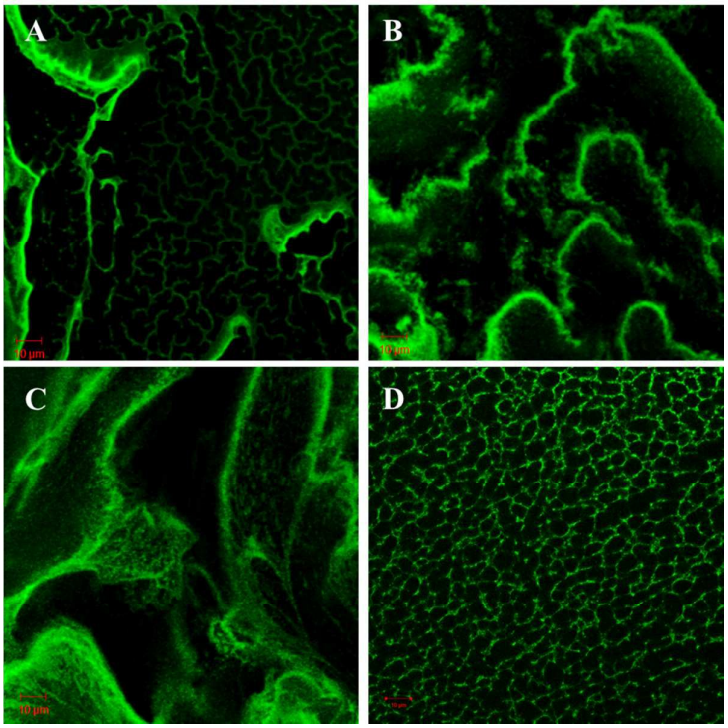

Fig. 5. Confocal microscopy of wet emulgels, chitosan concentration in all the

emulgels was 0.5 wt% and CA nanoemulsion contents varied: (A) 0.5%; (B) 1%; (C) 2%; (D) 5%

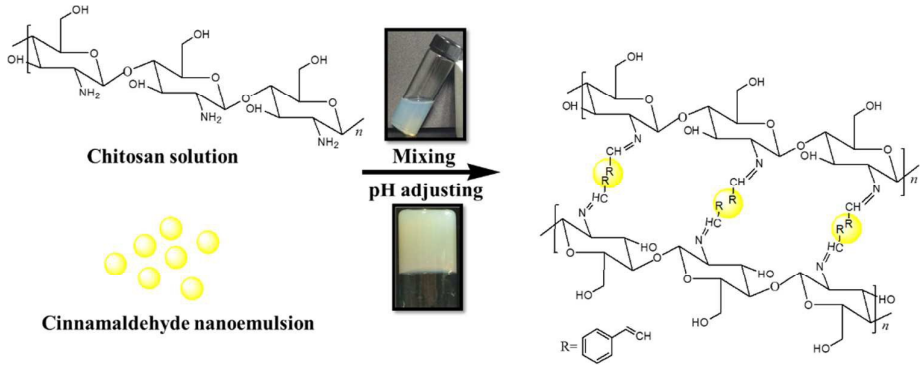

(A)

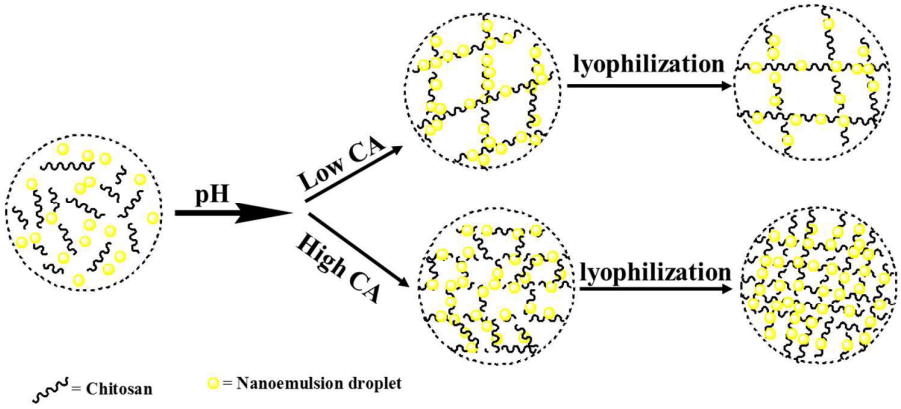

(B)

Fig. 6. Scheme of (A)chitosan and CA nanoemulsions emulgels Formation and (B) network microstructure of emulgels under different CA content and after freeze-drying

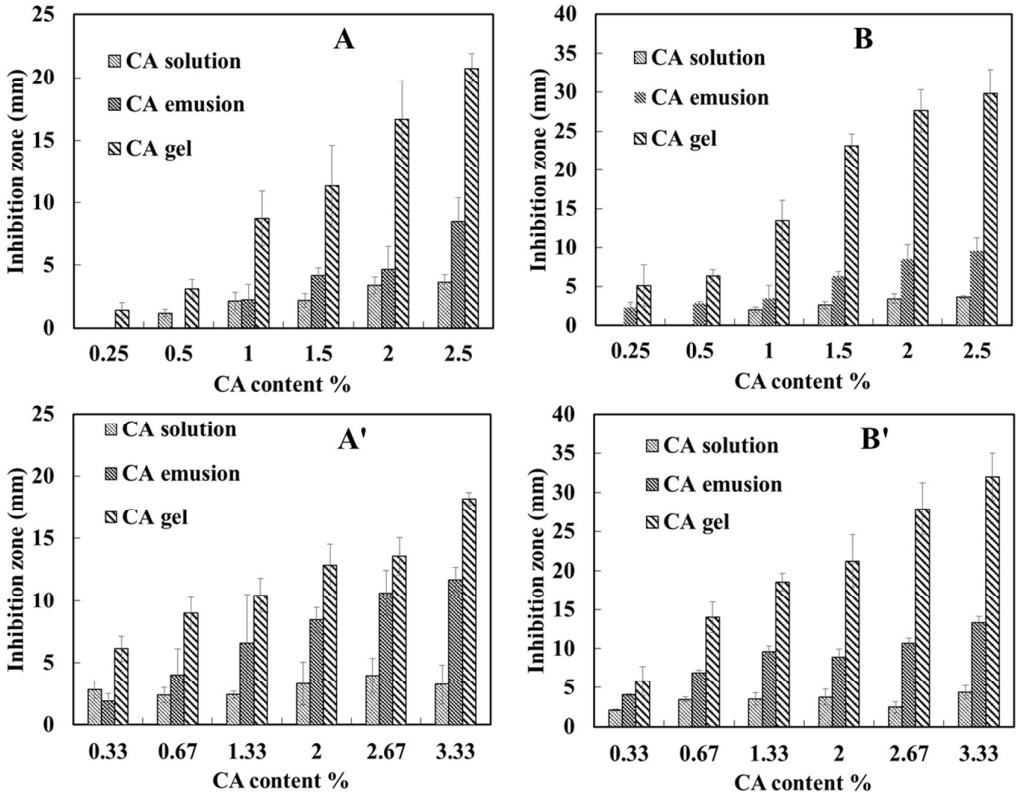

Fig. 7. Antibacterial activity against *E. coli* (A and A') and *S. aureus* (B and B') of emulgels with different amount of CA and MCT ratio in the formulation of nanoemulsions. A, B: the mass ratio of CA to MCT is 1:1, A' and B': the mass ratio of CA to MCT is 2:1

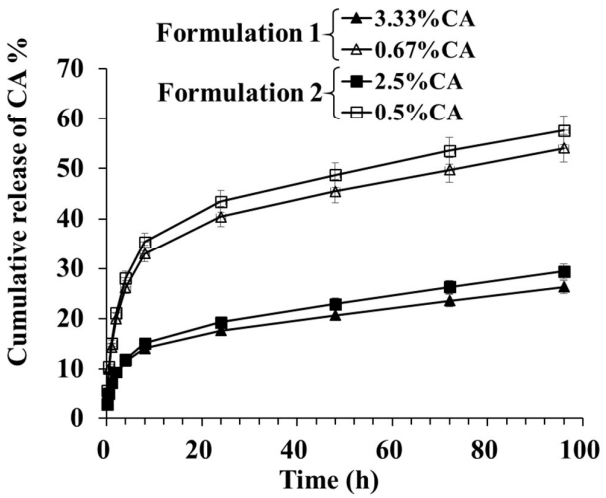

Fig. 8. Influence of CA level on the cumulative release of CA from chitosan emulgels containing different amount of CA and MCT ratio in the formulation of nanoemulsions. Formulation 1: the mass ratio of CA to MCT is 2:1, Formulation 2: the mass ratio of CA to MCT is 1:1